

# A New Tantalum Dinitrogen Complex and a Parahydrogen-Induced Polarization Study of Its Reaction with Hydrogen

Dawn C. Bregel, Susan M. Oldham, Rene J. Lachicotte, and Richard Eisenberg\*

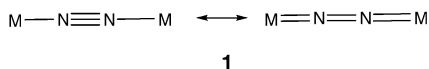
Department of Chemistry, University of Rochester, Rochester, New York 14627

Received March 8, 2002

Reduction of  $\text{Cp}^*_2\text{TaCl}_2$  with sodium amalgam in THF under a nitrogen atmosphere results in the formation of the novel complex  $(\text{Cp}^*_2\text{TaCl})_2(\mu\text{-N}_2)$ . This dinuclear complex containing a  $\mu\text{-}\eta^1\text{:}\eta^1$  dinitrogen bridge has been characterized by NMR and X-ray crystallography. The complex possesses a  $C_2$ -symmetric structure with each Ta bound to diastereotopic  $\text{Cp}^*$  rings and chloride in addition to the  $\mu\text{-N}_2$  bridge. The Ta–N and N–N distances of 1.885(10) and 1.23(1) Å, respectively, suggest modest reduction of the dinitrogen moiety. The two  $\text{Cp}^*$  resonances on each Ta center remain inequivalent in solution, even up to 80 °C. Addition of hydrogen results in the formation of two isomers of the dihydride complex  $\text{Cp}^*_2\text{TaH}_2\text{Cl}$ . Under parahydrogen, polarized resonances are observed for the unsymmetrical isomer with adjacent hydrides as the product of  $\text{H}_2$  oxidative addition. The symmetric isomer of  $\text{Cp}^*_2\text{TaH}_2\text{Cl}$  also forms, most likely by isomerization of the unsymmetrical kinetic isomer. The reactivity of  $(\text{Cp}^*_2\text{TaCl})_2(\mu\text{-N}_2)$  was compared to that of the related monomer,  $\text{Cp}^*_2\text{TaCl}(\text{THF})$ . The THF adduct yields the same hydrogen addition products, but the reaction is much more facile than for the nitrogen dimer, indicative of the structural integrity of the  $\mu\text{-N}_2$  complex.

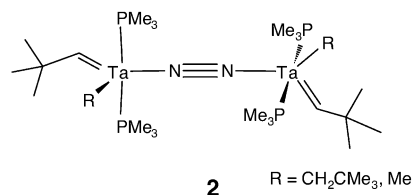
## Introduction

The challenge of activating dinitrogen is intimately related to the coordination chemistry of  $\text{N}_2$  as a ligand.<sup>1,2</sup> In this context, a number of different  $\text{N}_2$  bonding modes to metal centers have been characterized and metrical parameters from crystallographic studies have been analyzed to gauge the nature and extent of  $\text{N}\equiv\text{N}$  bond activation. For early metal systems, the most commonly encountered mode of dinitrogen coordination is as a bridge between two metal centers in an end-on, end-on or  $\mu\text{-}\eta^1\text{:}\eta^1$  manner. For a linear arrangement of this type, shown as **1**, different resonance structures have been invoked to reflect the extent of reduction based on M–N and N–N bond distances.



The first  $\text{N}_2$  complexes containing tantalum were reported in 1980 by Schrock, and are shown schematically as **2**.<sup>3</sup> The nearly linear Ta– $\text{N}_2$ –Ta arrangement was considered to give evidence of metal– $\text{N}_2$  back-bonding with an elongated N–N

distance of 1.30 Å and Ta–N bond distances of 1.84 Å. Subsequent studies of related complexes by Schrock and Churchill yielded structures similar to **2** with metrical parameters showing only slight variations.<sup>4,5</sup> More recent work by Fryzuk has revealed an interesting end-on, side-on or  $\mu\text{-}\eta^1\text{:}\eta^2$  mode of coordination in which reduction of the  $\text{N}_2$  may even be greater, although the occurrence of this bonding mode is linked to the presence of *other* bridging ligands.<sup>6</sup>



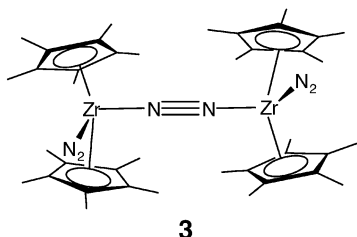
In the present study, we describe the synthesis of another dinuclear Ta– $\text{N}_2$ –Ta complex that is closely related to the

\* Author to whom correspondence should be addressed. E-mail: RES7@chem.rochester.edu.

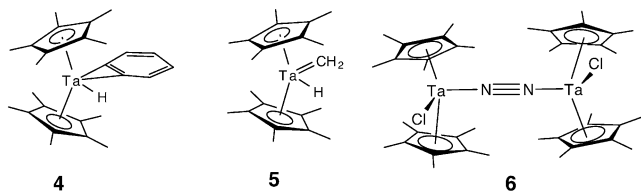
(1) Hidai, M.; Mizobe, Y. *Chem. Rev.* **1995**, *95*, 1115–1133.  
(2) Fryzuk, M. D.; Johnson, S. A. *Coord. Chem. Rev.* **2000**, *200*–202, 379–409.

(3) Turner, H. W.; Fellmann, J. D.; Rocklage, S. M.; Schrock, R. R.; Churchill, M. R.; Wasserman, H. J. *J. Am. Chem. Soc.* **1980**, *102*, 7809–7811.  
(4) Churchill, M. R.; Wasserman, H. J. *Inorg. Chem.* **1981**, *20*, 2899–2904.  
(5) Churchill, M. R.; Wasserman, H. J. *Inorg. Chem.* **1982**, *21*, 218–222.  
(6) Fryzuk, M. D.; Johnson, S. A.; Patrick, B. O.; Albinati, A.; Mason, S. A.; Koetzle, T. F. *J. Am. Chem. Soc.* **2001**, *123*, 3960–3973.

well-known dinitrogen complex of zirconium,  $\text{Cp}^*_4\text{Zr}_2(\text{N}_2)_3$  (**3**), first synthesized and studied by Bercaw.<sup>7</sup> Complex **3** has a structural arrangement that possesses overall  $C_2$  symmetry and diastereotopic  $\text{Cp}^*$  rings. The latter is evidenced by two signals for the  $\text{Cp}^*$  methyl protons in the  $^1\text{H}$  NMR spectrum at 4 °C.<sup>8</sup> The extent of reduction of the  $\mu\text{-N}_2$  ligand relative to the terminal dinitrogen ligands was thought to be significant and a bonding picture was formulated that involved pairwise  $\text{Zr}-(\mu\text{-N}_2)$  back-bonding. However, based on the N–N bond length of 1.18 Å for the bridging ligand, the extent of reduction appears to be less than that of the Ta systems exemplified by **2**.



Our foray into the chemistry presented in this paper derives from earlier work in which the activation of molecular hydrogen by pentamethylcyclopentadienyl ( $\text{Cp}^*$ ) Ta complexes such as **4** and **5** was being investigated with parahydrogen-induced polarization (PHIP).<sup>9</sup> In PHIP, pairwise addition of hydrogen can be definitively established by enhanced resonances of the product hydrogen nuclei that were formerly part of the  $\text{H}_2$  addend.<sup>10</sup> The specific question being probed was whether  $\text{H}_2$  addition to complexes such as **4** and **5** occurs via initial formation of a Ta(III) intermediate followed by metal-centered oxidative addition or by a single step mechanism involving a four-centered transition state. After establishment of the former for complex **4**, attention focused on the methylenide complex **5**. However, in the course of preparing **5**, a new Ta dinitrogen complex (**6**) was synthesized, characterized, and structurally analyzed. These results are described herein. The structure of **6** exhibits striking similarities to that of the dinuclear Zr complex **3**. Additionally, complex **6** was found to react with hydrogen, which in turn led to a PHIP study of the reaction and the identification of the reaction products.



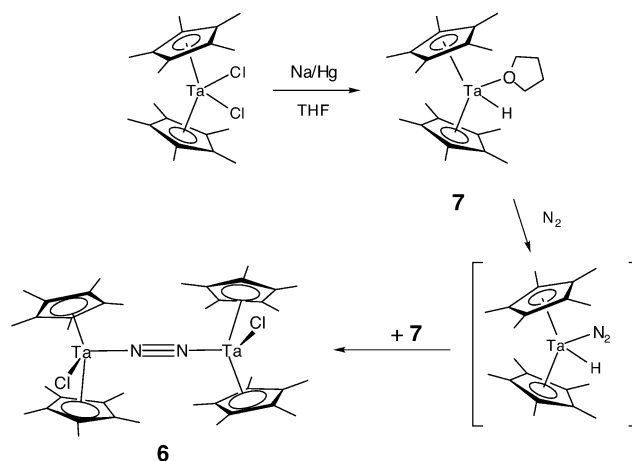
(7) Sanner, R. D.; Manriquez, J. M.; Marsh, R. E.; Bercaw, J. E. *J. Am. Chem. Soc.* **1976**, *98*, 8351–8358.

(8) Manriquez, J. M.; McAlister, D. R.; Rosenberg, E.; Shiller, A. M.; Williamson, K. L.; Chan, S. I.; Bercaw, J. E. *J. Am. Chem. Soc.* **1978**, *100*, 3078–3083.

(9) Millar, S. P.; Zubris, D. L.; Bercaw, J. E.; Eisenberg, R. *J. Am. Chem. Soc.* **1998**, *120*, 5329–5330.

(10) Duckett, S. B.; Sleight, C. J. *Prog. Nucl. Magn. Reson. Spectrosc.* **1999**, *23*, 71–92.

Scheme 1



## Results and Discussion

**Synthesis and Characterization of  $(\text{Cp}^*_2\text{TaCl})_2(\mu\text{-N}_2)$  (**6**).** Under a nitrogen atmosphere, addition of sodium amalgam to a solution of  $\text{Cp}^*_2\text{TaCl}_2$  in THF yields the nitrogen dimer complex  $(\text{Cp}^*_2\text{TaCl})_2(\mu\text{-N}_2)$  (**6**). When analyzed by  $^1\text{H}$  NMR spectroscopy, two inequivalent  $\text{Cp}^*$  resonances are observed in a 1:1 ratio at  $\delta$  1.88 and 1.96 (benzene- $d_6$ ). As observed by  $^1\text{H}$  and  $^{13}\text{C}$  NMR analyses, and supported by the crystal structure results described below, the  $\text{Cp}^*$  ligands contained on a single metal center are inequivalent. This inequivalence of the  $\text{Cp}^*$  resonances is maintained up to 80 °C (the highest temperature at which monitoring was possible), with no evidence of significant line broadening. This means that the overall  $C_2$  symmetry of the complex that renders the  $\text{Cp}^*$  rings on each Ta inequivalent (see below) is preserved and that hindered rotation about the  $\text{Ta-N}_2\text{-Ta}$  axis is maintained up to 80 °C.

The proposed rationale for the formation of complex **6** is shown in Scheme 1. From the literature, it is known that reduction of  $\text{Cp}^*_2\text{TaCl}_2$  by sodium amalgam yields the THF adduct  $\text{Cp}^*_2\text{TaCl}(\text{THF})$  (**7**).<sup>11</sup> Although not directly observed in our system, **7** is very likely an intermediate during the reaction to produce **6**. Reactions that generated complex **6** were carried out in a dinitrogen-filled glovebox. Under these conditions, intermediate **7** would react rapidly with dinitrogen to form  $\text{Cp}^*_2\text{TaCl}(\text{N}_2)$  that would in turn displace THF from another molecule of **7** to yield **6**.

Previous reports from the Bercaw laboratory identified a spectroscopically ( $^1\text{H}$  NMR) identical red species that formed after the monochloride THF adduct,  $\text{Cp}^*_2\text{TaCl}(\text{THF})$  (**7**), was allowed to stand at room temperature for several hours.<sup>11</sup> The red product was proposed to be a dimer or oligomer described by the empirical formula  $[\text{Cp}^*_2\text{TaCl}]_n$ , consistent with elemental analyses. It is likely that the red species previously reported is actually the nitrogen dimer **6** that formed slowly under an atmosphere containing a much smaller amount of dinitrogen.

(11) Antonelli, D. M.; Schaefer, W. P.; Parkin, G.; Bercaw, J. E. *J. Organomet. Chem.* **1993**, *462*, 213–220.

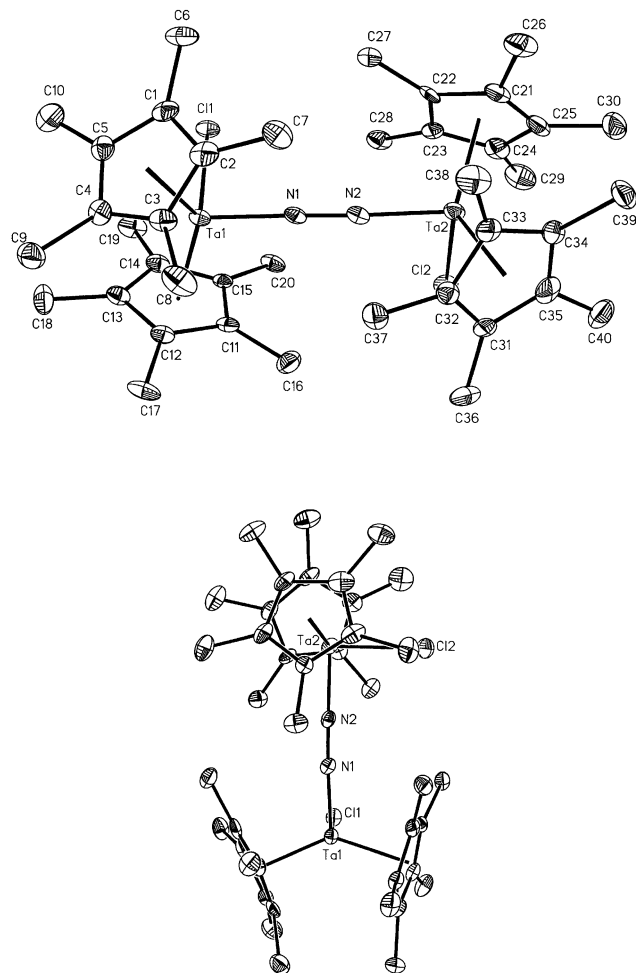


**Figure 1.** (Top) An ORTEP representation of  $[\text{Cp}^*_2\text{TaCl}]_2(\mu\text{-N}_2)$  (**6**) showing 50% probability ellipsoids. For clarity, H atoms are not shown. (Bottom) A view clearly showing the orthogonal orientation of the two  $\text{TaCp}_2\text{Cl}$  moieties.

**Structure Determination of 6.** Red needles suitable for X-ray analysis were obtained by slow diffusion of pentane into a concentrated THF solution of **6**. The X-ray analysis shows that **6** is a dimer of two  $\text{Cp}^*_2\text{TaCl}$  fragments that are bridged by an end-on bound, or  $\mu\text{-}\eta^1\text{:}\eta^1$ , dinitrogen ligand. An ORTEP representation of **6** is shown in Figure 1. Crystallographic, data collection, and refinement information are summarized in Table 1. Selected bond lengths and angles are listed in Table 2. The N–N bond length is 1.235(13) Å, which is significantly longer than that of free  $\text{N}_2$  (1.0976 Å). The Ta–N–N–Ta moiety is nearly linear, with an average Ta–N–N angle of 176.7(8)° and an average Ta–N bond length of 1.885(10) Å. Figure 2 depicts two skeletal views, side-on and along the Ta–N–N–Ta axis, revealing the torsion angles. For simplicity, the  $\text{Cp}^*$  ligands are omitted and the centroids, labeled R(1), R(2), R(3), and R(4), are shown. The chloride ligand on Ta(1) eclipses one of the  $\text{Cp}^*$  ligands on Ta(2). The torsion angle between the two chloride ligands is 91.8°, and the plane of R(1)–Ta(1)–R(2) is nearly orthogonal to that of R(3)–Ta(2)–R(4), with a torsion angle of 75.5°. The only symmetry element found in **6** is a  $C_2$  rotation axis, which bisects the N–N bond and a line connecting the two terminal chloride ligands. This  $C_2$  axis relates

**Table 1.** Crystal and Structure Refinement Data for **6**

crystal parameters	
chemical formula	$\text{C}_{42}\text{H}_{64}\text{Cl}_2\text{N}_2\text{O}_{0.5}\text{Ta}_2$
fw	1037.75
cryst syst	monoclinic
space group (no.)	$P2_1/n$ (no. 14)
Z	4
a, Å <sup>a</sup>	9.2650(2)
b, Å	28.1964(4)
c, Å	19.0302(3)
β, deg	99.337(1)
vol, Å <sup>3</sup>	4905.6(2)
ρ <sub>calc</sub> , mg/m <sup>3</sup>	1.405
crystal dims, mm	0.36 × 0.18 × 0.04
temp, °C	–80
measurement of intensity data	
diffractometer	Siemens SMART
radiation, λ, Å	Mo, 0.71073
2θ range for data collection, deg	3.62–46.9
limiting indices	–10 ≤ h ≤ 10, –31 ≤ k ≤ 23, –21 ≤ l ≤ 19
total reflns to 45° <sup>b</sup>	20417
independent reflns	7006 [R(int) = 0.0632]
no. of obsd data	5325 (I > 2σ(I))
no. of params varied	430
μ, mm <sup>–1</sup>	4.593
abs corr	empirical (SADABS) <sup>c</sup>
range of trans. factors	0.378–0.928
goodness-of-fit on F <sup>2d</sup>	1.091
R <sub>1</sub> (F <sub>o</sub> ) (%) <sup>e</sup>	4.58
wR <sub>2</sub> (F <sub>o</sub> <sup>2</sup> ) (I > 2σ(I)) (%) <sup>e</sup>	14.86
R <sub>1</sub> (F <sub>o</sub> ) (all data) (%) <sup>e</sup>	6.98
wR <sub>2</sub> (F <sub>o</sub> <sup>2</sup> ) (all data) (%) <sup>e</sup>	15.71
abs structure param	–0.021(8)

<sup>a</sup> It has been noted that the integration program SAINT produces cell constant errors that are unreasonably small, since systematic error is not included. More reasonable errors might be estimated at 10× the listed value. Data greater than 45° were omitted from the refinement. <sup>b</sup>  $R_{\text{int}} = \sum |F_o^2 - F_c^2(\text{mean})| / \sum F_o^2$ ;  $R_{\text{sig}} = \sum [\sigma(F_o^2)] / \sum F_o^2$ . <sup>c</sup> The SADABS program is based on the method of Blessing; see: Blessing, R. H. *Acta Crystallogr., Sect. A* **1995**, 51, 33. <sup>d</sup>  $\text{GOF} = [\sum (w(F_o^2 - F_c^2)^2) / (n - p)]^{1/2}$ , where n and p denote the number of data and parameters. <sup>e</sup>  $R_1 = (\sum ||F_o| - |F_c||) / \sum |F_o|$ ;  $wR_2 = [\sum (w(F_o^2 - F_c^2)^2) / \sum (w(F_o^2)^2)]^{1/2}$ , where  $w = 1 / [\sigma^2(F_o^2) + (a \cdot P)^2 + b \cdot P]$  and  $P = [(\max(0, F_o^2) + 2 \cdot F_c^2)] / 3$ .

**Table 2.** Selected Bond Lengths (Å) and Angles (deg) for **6**

N(1)–N(2)	1.235(13)	Ta(1)–C(4)	2.467(12)
Ta(1)–N(1)	1.878(10)	Ta(1)–C(5)	2.464(12)
Ta(2)–N(2)	1.892(10)	Ta(1)–C(11)	2.408(11)
Ta(1)–Cl(1)	2.442(3)	Ta(1)–C(12)	2.465(11)
Ta(2)–Cl(2)	2.458(3)	Ta(1)–C(13)	2.553(11)
Ta(1)–C(1)	2.512(12)	Ta(1)–C(14)	2.493(12)
Ta(1)–C(2)	2.521(12)	Ta(1)–C(15)	2.406(11)
Ta(1)–C(3)	2.442(12)		
Ta(1)–N(1)–N(2)	177.0(8)	N(1)–Ta(1)–Cl(1)	90.2(3)
Ta(2)–N(2)–N(1)	176.3(8)	N(2)–Ta(2)–Cl(2)	90.0(3)

the two chloride ligands on the two metal centers as well as the two pairs of  $\text{Cp}^*$  ligands.

**Comparison to Other Nitrogen Dimers.** Complex **6** is one of relatively few tantalum dinitrogen dimers that have been crystallographically characterized.<sup>4–6,12</sup> The Ta–N bond lengths for other tantalum dinitrogen complexes range from 1.796(5) to 1.842(8) Å, while N–N bond lengths range from 1.282(6) to 1.32(1) Å. In all these Ta–N<sub>2</sub>–Ta complexes, the N–N bond order is somewhere between 2 (N=N is 1.24 Å) and 1 (N–N is 1.45 Å).<sup>4</sup> By comparison, complex **6** has

(12) Schrock, R. R.; Wesolek, M.; Liu, A. H.; Wallace, K. C.; Dewan, J. C. *Inorg. Chem.* **1988**, 27, 2050–2054.

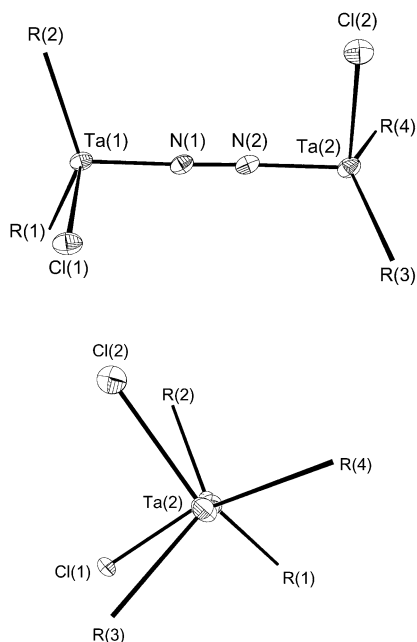


**Figure 2.** Skeletal depictions of  $[\text{Cp}^*_2\text{TaCl}]_2(\mu\text{-N}_2)$  (**6**) as viewed from the side and along the Ta–N–N–Ta axis, revealing the torsion angles. The Cp\* rings are omitted and the centroids are labeled R(1), R(2), R(3), and R(4).

longer Ta–N bond distances and a shorter N–N bond distance, which translates into a less reduced dinitrogen ligand with a N–N bond order close to 2. In terms of bond angles, the majority of the known tantalum dinitrogen dimer complexes contain a linear Ta–N–N–Ta moiety, as is observed for **6**.

The torsion angles for **6** can be compared to those given for the Schrock complex  $[\text{Ta}(=\text{CHCMe}_3)(\text{CH}_2\text{CMe}_3)(\text{PMe}_3)_2]_2(\mu\text{-N}_2)$  (**2**).<sup>4</sup> The angle between the equatorial coordination planes (consisting of  $\text{CHCMe}_3$ ,  $\text{CH}_2\text{CMe}_3$ , Ta, and N) for each tantalum atom of complex **2** is  $82.59^\circ$ . In other words, the two equatorial planes are nearly perpendicular. As mentioned above, the two Cl–Ta–N planes for **6** are very nearly perpendicular ( $91.8^\circ$ ), while the equatorial planes consisting of one tantalum and two Cp\* centroids are close to perpendicular, with an angle of  $75.5^\circ$ . For both complexes, the perpendicular orientation of the two tantalum fragments surrounding the dinitrogen ligand can be explained in terms of orbital overlap. If the dinitrogen moiety is considered as a neutral ligand, then each tantalum center is Ta(III) which is  $d^2$ . One Ta–N<sub>2</sub>  $\pi$  interaction can be described as back-donation from a filled  $d_{xz}$  orbital of one metal center into the dinitrogen  $\pi^*_x$  orbital, while the other Ta–N<sub>2</sub>  $\pi$  interaction results from similar back-donation from the second metal ion into the dinitrogen  $\pi^*_y$  orbital. This explains both the observed perpendicular orientation of the two tantalum fragments and the reduction in bond order of the dinitrogen moiety based on  $\pi$  back-bonding interactions.

The known tantalum dinitrogen complexes do not closely resemble **6** in terms of overall structure. However, the related zirconium dinitrogen complex,  $(\text{Cp}^*_2\text{ZrN}_2)_2(\mu\text{-N}_2)$  (**3**), provides an opportunity for a close comparison.<sup>7</sup> The zirconium complex is formally isoelectronic with **6** and is also structur-

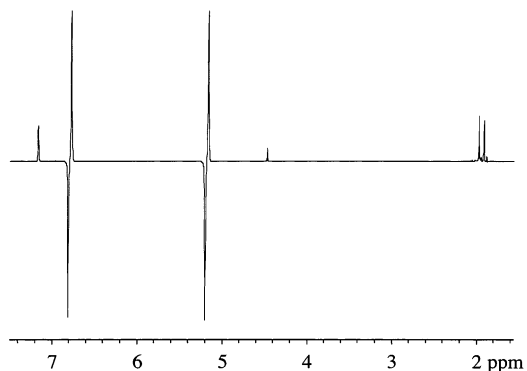


**Figure 3.**  $^1\text{H}$  NMR spectrum of  $(\text{Cp}^*_2\text{TaCl})_2(\mu\text{-N}_2)$  (**6**) in the presence of para-enriched hydrogen in benzene- $d_6$  at  $75^\circ\text{C}$ .

ally related, containing a terminal N<sub>2</sub> ligand on each metal fragment rather than a terminal chloride ligand. The bridging N–N bond distance in the zirconium complex is  $1.182(5)$  Å, compared to  $1.235(13)$  Å in **6**. The torsion angle between terminal nitrogen ligands on different zirconium centers is  $87.3^\circ$ , which compares well with the  $91.8^\circ$  angle between the chlorides on each tantalum center of **6**. The bonding analysis given in the preceding paragraph is in fact essentially the same as that offered by Bercaw for **3** to explain its observed structure.<sup>7</sup>

While **3** and **6** are structurally similar, there is a significant difference in the temperature required for fluxionality of the Cp\* ligands of each complex. For **6**, the Cp\* ligands contained on a single metal center are inequivalent, and this is maintained at elevated temperatures (measured up to  $80^\circ\text{C}$ ). A consequence of this observation is that the C<sub>2</sub> symmetry of **6** is preserved and rotation about the Ta–N<sub>2</sub>–Ta axis remains hindered up to this temperature. In contrast, **3** reveals inequivalent Cp\* resonances only below  $4^\circ\text{C}$ . In this case, reversible dissociation of the terminal N<sub>2</sub> ligands may provide a facile pathway to exchange the Cp\* ligands on the NMR time scale.<sup>8</sup>

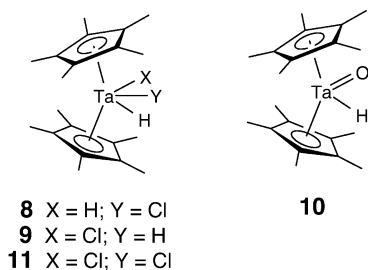
**Reaction of  $(\text{Cp}^*_2\text{TaCl})_2(\mu\text{-N}_2)$  (**6**) with Dihydrogen.** In benzene- $d_6$ , addition of hydrogen to **6** shows little reactivity at room temperature. However, within several hours of heating at  $60^\circ\text{C}$ , all starting material is consumed and several new products are observed. In all cases, two new Cp\* resonances are observed at  $\delta$  1.91 and 1.85, approximately equal in intensity, along with other, less intense resonances at  $\delta$  7.1 (singlet), 6.7 (doublet,  $J_{\text{H-H}} = 15$  Hz), and 5.1 (doublet,  $J_{\text{H-H}} = 15$  Hz). In some of the experiments, two additional products are observed, with Cp\* resonances at  $\delta$  1.94 and 1.83 and smaller peaks at  $\delta$  12.2 (singlet) and 7.4 (singlet).

The addition of parahydrogen to **6** in benzene- $d_6$  leads to polarized resonances at  $\delta$  6.7 and 5.1 (emission/absorption doublets,  $J_{\text{H-H}} = -15$  Hz). The resonances are apparent at  $30^\circ\text{C}$ , but only at low intensity whereas the polarization is very intense at elevated temperatures. With the NMR probe at  $75^\circ\text{C}$ , enhancement of greater than 1000-fold is observed (Figure 3). Heating several hours at  $60^\circ\text{C}$  (in an oil bath) pushes the reaction with hydrogen to completion, with no remaining resonances for **6**. Normal doublets are observed

for the resonances at  $\delta$  6.7 and 5.1. There are also the same resonances at  $\delta$  7.1, 1.91, and 1.85 observed with normal hydrogen.

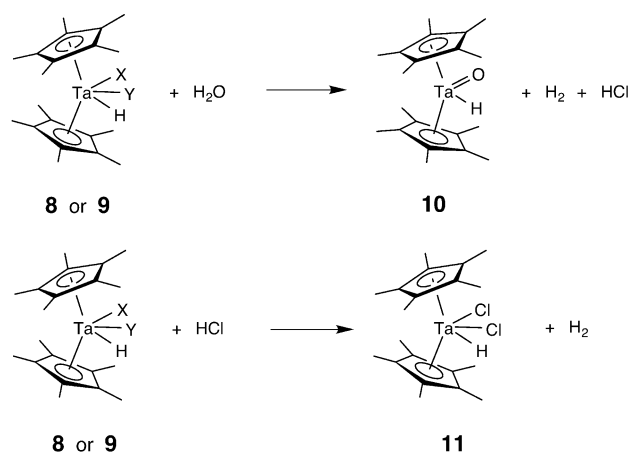
Similar reactivity is observed for the addition of parahydrogen to **6** in THF- $d_8$ . Intense polarized resonances at  $\delta$  6.3 and 5.1 (emission/absorption doublets,  $J_{H-H} = -15$  Hz) are observed at 75 °C. After additional heating at 60 °C (several hours), the reaction goes to completion to yield approximately equal amounts of Cp\* resonances at  $\delta$  2.04 and 1.93, with smaller resonances at 6.8 (singlet), 6.3 (doublet,  $J_{H-H} = 15$  Hz), and 5.1 (doublet,  $J_{H-H} = 15$  Hz).

The various products for the reaction of **6** with hydrogen in benzene- $d_6$  are assigned by using the literature and the results of the experiments described above. From the literature, it is found that the resonances at  $\delta$  1.91 and 7.1 correspond to the symmetrical dihydride complex Cp\*<sub>2</sub>TaH<sub>2</sub>Cl (**8**) with chloride in the central position and hydrides in the lateral positions of the bent metallocene structure.<sup>13</sup> Integration shows a ratio of 15:1. Based on this and the results of the parahydrogen experiment, the resonances at  $\delta$  1.85, 6.7, and 5.1, which integrate as 30:1:1, are assigned to the unsymmetrical isomer of Cp\*<sub>2</sub>TaH<sub>2</sub>Cl (**9**) with hydrides adjacent to each other in lateral and central positions. Dihydride **9** is the only isomer that would exhibit polarization since PHIP requires that pairwise addition of dihydrogen results in nonequivalent proton sites in the product.



As mentioned above, in some of the reactions of **6** with hydrogen in benzene- $d_6$ , additional products are formed. One of these is Cp\*<sub>2</sub>Ta(=O)H (**10**), with the Cp\* resonance at  $\delta$  1.94 and the hydride at  $\delta$  7.4, assigned by comparison to literature NMR data and confirmed by integration (30:1).<sup>14</sup> Tantalum species often react rapidly with water, and the common product of water addition to tantalocene complexes is **10**.<sup>11,14</sup> The other product, also assigned based on literature NMR data, is the dichloride complex Cp\*<sub>2</sub>TaHCl<sub>2</sub> (**11**), with the Cp\* resonance at  $\delta$  1.83 and the hydride at  $\delta$  12.2 (integrate as 30:1).<sup>13</sup> Formation of **11** appears to correlate with the presence of water and the observation of **10** (in reactions with observable signals for **11**, there is always a significant amount of **10** present). As shown in Scheme 2, the formation of **11** may be due to initial formation of **10** by reaction of **8** or **9** with water. Formation of **10** results in elimination of HCl, which is known to react with **8** (and likely **9**) to form **11**.<sup>13</sup> Indeed, when water is added to a

Scheme 2



sample of **8** and **9** in benzene- $d_6$ , signals for **10** and **11** are observed by NMR spectroscopy.

The products formed upon addition of hydrogen to **6** in THF- $d_8$  are identical with those formed in benzene- $d_6$ , with slight variations in chemical shift. The symmetrical dihydride Cp\*<sub>2</sub>TaH<sub>2</sub>Cl (**8**) appears at  $\delta$  2.04 and 6.7 (integrate as 15:1), while isomer **9** exhibits resonances at  $\delta$  1.93 for Cp\* and at  $\delta$  6.3 and 5.1 for the hydrides with integrations of 30:1:1. The polarized resonances observed in the reaction with parahydrogen correspond to those of complex **9**. After the reaction with hydrogen goes to completion, the two Cp\*<sub>2</sub>TaH<sub>2</sub>Cl isomers are present in approximately equal amounts (<sup>1</sup>H NMR).

From the hydrogen addition studies, it appears that the nitrogen complex **6** reacts with 2 equiv of H<sub>2</sub> to yield a dihydride species, Cp\*<sub>2</sub>TaH<sub>2</sub>Cl, which is present as two isomers, **8** and **9**. The question remains, by what mechanism does H<sub>2</sub> react with **6**? The two most likely possibilities are direct addition of H<sub>2</sub> to a tantalum metal center of **6**, followed by cleavage of the dinuclear complex, or slow and unobserved cleavage of the dimer into Cp\*<sub>2</sub>TaCl and Cp\*<sub>2</sub>TaCl(N<sub>2</sub>) fragments, followed first by reaction of the coordinatively unsaturated moiety Cp\*<sub>2</sub>TaCl with H<sub>2</sub> and then by loss of N<sub>2</sub> from Cp\*<sub>2</sub>TaCl(N<sub>2</sub>) and another addition of H<sub>2</sub>.

To gain insight into the mechanism, the reactivity of **6** is compared to that of the Ta(III) precursor Cp\*<sub>2</sub>TaCl(THF- $d_8$ ) (**7**).<sup>11</sup> Complex **7** is prepared under nitrogen-free conditions to avoid formation of **6**, and then the reaction with hydrogen in THF- $d_8$  is examined. The addition of hydrogen to **7** yields the same hydrogen addition products as observed with **6**, but much more rapidly. After 1 h at room temperature, Cp\*<sub>2</sub>TaH<sub>2</sub>Cl (**9**) is the only species present by NMR spectroscopy. After several hours at room temperature, the formation of the symmetrical isomer Cp\*<sub>2</sub>TaH<sub>2</sub>Cl (**8**) is observed, likely by isomerization of the initially formed dihydride **9**. While the addition of H<sub>2</sub> to **7** is complete within 1 h at room temperature, the reaction of **6** with H<sub>2</sub> requires several hours of heating at 60 °C, which points to a mechanism of preliminary dimer cleavage.

Additional support for the dimer cleavage mechanism comes from the reaction of **6** with CO in benzene- $d_6$ . The sole product is the monomeric complex Cp\*<sub>2</sub>Ta(CO)Cl (**12**),

(13) Shin, J. H.; Parkin, G. *Organometallics* **1998**, *17*, 5689–5696.

(14) van Asselt, A.; Burger, B. J.; Gibson, V. C.; Bercaw, J. E. *J. Am. Chem. Soc.* **1986**, *108*, 5347–5349.

which is a known species.<sup>11</sup> The reaction proceeds rather slowly, with only 25% of **6** converted to **12** after 18 h at room temperature (by NMR). Complete conversion is achieved only after heating at 45 °C for 8 h. In comparison, the monomeric THF complex **7** has been reported to react with CO to yield **12** in only 2 h at room temperature.<sup>11</sup>

On the basis of the experiments described above, a mechanism involving slow and unobserved cleavage of the dinuclear complex **6** into Cp\*<sub>2</sub>TaCl and Cp\*<sub>2</sub>TaCl(N<sub>2</sub>) fragments, followed by reaction with H<sub>2</sub>, is favored over a pathway of direct addition of H<sub>2</sub> to a saturated, 18 e<sup>-</sup> tantalum metal center of **6**, followed by cleavage of the dimer. In comparing the reactivity of **6** and the related monomer **7** with both H<sub>2</sub> and CO, it is obvious that an increase in the accessibility of [Cp\*<sub>2</sub>TaCl] clearly has a significant effect on the reactivity. Although CO does react slightly more rapidly with **6** than does H<sub>2</sub>, both reactions are very slow compared to those of **7**. Essentially, the comparatively slower reactions of **6** can be attributed to the structural integrity and stability of the μ:η<sup>1</sup>-η<sup>1</sup> N<sub>2</sub> bridge, relative to the more facile reactions of **7** that result from the lability of THF.

In the reaction of **6** with H<sub>2</sub>, the unsymmetrical dihydride **9**, formed by pairwise cis addition, is likely the initial product, followed by isomerization to yield **8**. As a potential verification of this notion, the reaction was monitored by NMR spectroscopy at 1-h intervals (60 °C, THF-*d*<sub>8</sub>). However, it was found that at all times measured (1 to 5 h), **8** and **9** are present in approximately equal amounts. Even at the lower temperature of 40 °C, **8** and **9** appear at approximately the same rate. For this result to be consistent with the notion of initial formation of **9** followed by isomerization to **8**, the isomerization has to be competitive with dimer cleavage and subsequent H<sub>2</sub> addition. Two alternative mechanisms for the formation of **8** are as follows: (1) a stepwise or non-cis addition pathway for the addition of H<sub>2</sub> to **6** and (2) formation of **8** via a protonolysis mechanism, since **10** and **11** are often observed in the reactions. With regard to the latter, both **8** and **9** are often observed when **10** and **11** are not present, indicating that protonolysis is an unlikely pathway. While a stepwise addition cannot be ruled out at present, we favor a pathway involving initial formation of **9** as the kinetic isomer followed by isomerization of **9** to yield **8**. This mechanism receives strong support from the reaction of H<sub>2</sub> with Cp\*<sub>2</sub>TaCl(THF-*d*<sub>8</sub>) (**7**), which initially yields only **9** at room temperature, followed by the appearance of **8**.

## Conclusion

The novel tantalum dinitrogen dimer (Cp\*<sub>2</sub>TaCl)<sub>2</sub>(μ-N<sub>2</sub>) (**6**) has been prepared. Complex **6** was crystallographically characterized, and is one of only a handful of examples of tantalum dinitrogen dimers in the literature. Unlike the related zirconium complex, (Cp\*<sub>2</sub>ZrN<sub>2</sub>)<sub>2</sub>(μ-N<sub>2</sub>) (**3**), **6** is not fluxional, even at elevated temperatures. The nitrogen dimer **6** shows reactivity with H<sub>2</sub> to yield the isomeric Cp\*<sub>2</sub>TaH<sub>2</sub>Cl dihydride products **8** and **9**. The assignment of **9**, a novel species, was made possible by parahydrogen-induced polarization

studies. Very large polarization (enhancement of ca. 1000-fold) was observed for complex **9**. In the presence of water, two more products, Cp\*<sub>2</sub>Ta(=O)H (**10**) and Cp\*<sub>2</sub>TaHCl<sub>2</sub> (**11**), are also detected. The formation of **11** is likely due to reaction of **8** and **9** with HCl produced in the formation of **10**. The monomeric complex Cp\*<sub>2</sub>TaCl(THF) (**7**) reacts with H<sub>2</sub> to yield the same dihydrogen addition products as **6**, but much more rapidly. This difference in reactivity can be attributed to the structural integrity of (Cp\*<sub>2</sub>TaCl)<sub>2</sub>(μ-N<sub>2</sub>) (**6**) and stability of the μ:η<sup>1</sup>-η<sup>1</sup> N<sub>2</sub> bridge, relative to the lability of THF in Cp\*<sub>2</sub>TaCl(THF) (**7**).

## Experimental Section

**General Information.** All complexes were prepared with standard inert-atmosphere Schlenk, vacuum line, and drybox techniques. Solvents were dried with use of Grubb's purification system. Deuterated solvents were transferred from ampules to activated sieves and stored in the glovebox. Cp\*<sub>2</sub>TaCl<sub>2</sub> was prepared as previously reported.<sup>15</sup> Parahydrogen was prepared by cooling high-purity hydrogen over FeCl<sub>3</sub> adsorbed onto silica at 77 K.<sup>16</sup> All NMR spectra were recorded on a Bruker Avance-400 spectrometer. <sup>1</sup>H NMR chemical shifts are referenced relative to the residual proton peak(s) of deuterated solvents. Elemental analyses were obtained from Desert Analytics, Tucson, AZ.

**Preparation of (Cp\*<sub>2</sub>TaCl)<sub>2</sub>(μ-N<sub>2</sub>) (**6**).** In a typical experiment, Cp\*<sub>2</sub>TaCl<sub>2</sub> (250 mg, 0.475 mmol) and freshly prepared Na/Hg (11 mg, 0.475 mmol of Na in 0.5 mL of Hg) were added to a round-bottom flask in a nitrogen atmosphere drybox. To this was added 25 mL of THF. The green-brown suspension turned to yellow brown in a few minutes, and then gradually became red orange within 10 min. The mixture was allowed to stir for 1 h. The blood-red solution was then filtered through a plug of Celite and the solvent was removed in vacuo. The red solid was then recrystallized from diethyl ether and pentane to give red crystals. <sup>1</sup>H NMR (benzene-*d*<sub>6</sub>): δ 1.88 (s, C<sub>5</sub>(CH<sub>3</sub>)<sub>5</sub>), 1.96 (s, C<sub>5</sub>(CH<sub>3</sub>)<sub>5</sub>). <sup>13</sup>C NMR (benzene-*d*<sub>6</sub>): δ 11.7 (s, C<sub>5</sub>(CH<sub>3</sub>)<sub>5</sub>), 12.1 (s, C<sub>5</sub>(CH<sub>3</sub>)<sub>5</sub>), 113.8 (s, C<sub>5</sub>(CH<sub>3</sub>)<sub>5</sub>), 114.7 (s, C<sub>5</sub>(CH<sub>3</sub>)<sub>5</sub>). Anal. Calcd for C<sub>40</sub>H<sub>60</sub>N<sub>2</sub>Cl<sub>2</sub>Ta<sub>2</sub>: C, 47.96; H, 6.04; N, 2.80. Found: C, 47.51; H, 5.85; N, 3.15.

**Crystal Structure of **6**.** Crystals of **6** were grown by slow diffusion of pentane into a concentrated THF solution of **6**. A single red plate (approximate dimensions 0.36 × 0.18 × 0.04 mm<sup>3</sup>) was mounted on a glass fiber under Paratone-8277 and immediately placed on the X-ray diffractometer in a cold nitrogen stream at -80 °C. The X-ray intensity data were collected on a standard Siemens SMART CCD Area Detector System equipped with a normal focus molybdenum-target X-ray tube operated at 2.0 kW (50 kV, 40 mA). A total of 1321 frames of data (1.3 hemispheres) were collected by using a narrow frame method with scan widths of 0.3° in ω and exposure times of 30 s/frame with a detector-to-crystal distance of 5.09 cm (maximum 2θ angle of 56.6°). The total data collection time was approximately 13 h. Frames were integrated to a maximum 2θ angle of 46.9° with the Siemens SAINT program to yield a total of 20417 reflections, of which 7006 were independent (*R*<sub>int</sub> = 6.32%, *R*<sub>sig</sub> = 7.36%) (see Table 1 footnotes for formulas) and 5325 were above 2σ(*I*). Laue symmetry revealed a monoclinic crystal system, and the final unit cell parameters (at -80 °C) were determined from the least-squares refinement of

(15) Gibson, V. C.; Bercaw, J. E.; Bruton, W. J., Jr.; Sanner, R. D. *Organometallics* **1986**, *5*, 976–979.

(16) Millar, S. P.; Jang, M.; Lachicotte, R. J.; Eisenberg, R. *Inorg. Chim. Acta* **1998**, *270*, 363–375.

three-dimensional centroids of 8192 reflections. Data were corrected for absorption with the SADABS program.<sup>17</sup>

The space group was assigned as  $P2_1/n$  and the structure was solved by using direct methods and refined by employing full-matrix least-squares on  $F^2$ .<sup>18</sup> All of the non-hydrogen atoms were refined anisotropically, and the hydrogen atoms were included in idealized positions. What is best modeled as a diffuse THF molecule was located in the asymmetric unit. Although the elemental analysis of this material shows no residual THF, the five residual peaks refined well as a half-occupied THF molecule. The five atoms were left as carbon atoms and because it was impossible to differentiate one of them as an oxygen atom, the hydrogen atoms were not included. The final data<sub>obs</sub>:parameter ratio was >10:1. The structure refined to a goodness of fit (GOF) of 1.091 and final residuals of  $R_1 = 4.58\%$  ( $I > 2\sigma(I)$ ),  $wR_2 = 14.86\%$  ( $I > 2\sigma(I)$ ) (see Table 1 footnotes for formulas). Data collection and refinement parameters, all atomic coordinates, anisotropic displacement parameters, and bond distances and angles are presented in Supporting Information in CIF format.

**Addition of Hydrogen to  $(Cp^*_2TaCl)_2(\mu-N_2)$  (**6**).** In a typical experiment, a resealable NMR tube with a J. Young valve was charged with **6** (ca. 1–3 mg) and dry solvent (benzene- $d_6$  or THF- $d_8$ , ca. 0.5 mL) in a nitrogen atmosphere glovebox. The tube was frozen in liquid nitrogen and evacuated on a high-vacuum line, then hydrogen (ca. 1 atm) or para-enriched hydrogen (ca. 3 atm) was added to the tube. The reaction was monitored by  $^1H$  NMR spectroscopy and heated in an oil bath at 60 °C to complete the addition of hydrogen. Products in benzene- $d_6$ :  $Cp^*_2TaH_2Cl$  (**8**) [ $\delta$  1.91 (s, 30H,  $C_5CH_3$ ), 7.1 (s, 2H, Ta–H)],  $Cp^*_2TaH_2Cl$  (**9**) [ $\delta$  1.85 (s, 30H,  $C_5CH_3$ ), 6.7 and 5.1 (d,  $J_{H-H} = 15$  Hz, 2H, Ta–H)], and sometimes  $Cp^*_2Ta(=O)H$  (**10**) [ $\delta$  1.94 (s, 30H,  $C_5CH_3$ ), and 7.4 (s, 1H, Ta–H)] and  $Cp^*_2TaHCl_2$  (**11**) [ $\delta$  1.83 (s, 30H,  $C_5CH_3$ ), and 12.2 (s, 1H, Ta–H)]. NMR data for **8**, **10**, and **11** match those reported in the literature.<sup>13,14</sup> Products in THF- $d_8$ :  $Cp^*_2TaH_2Cl$  (**8**) [ $\delta$  2.04 (s, 30H,  $C_5CH_3$ ), 6.7 (s, 2H, Ta–H)],  $Cp^*_2TaH_2Cl$  (**9**) [ $\delta$  1.93 (s, 30H,  $C_5CH_3$ ), 6.3 and 5.1 (d,  $J_{H-H} = 15$  Hz, 2H, Ta–H)]. Assignments of products in THF- $d_8$  were made by comparison to benzene- $d_6$  spectra and integration of THF- $d_8$  spectra.

**Preparation of  $Cp^*_2TaCl(THF-d_8)$  (**7**).** The preparation of this complex has been previously reported by Bercaw and co-workers, but under slightly different conditions.<sup>11</sup> It was important to ensure

that no nitrogen was present. A resealable NMR tube with a J. Young valve was charged with  $Cp^*_2TaCl_2$  (2.0 mg, 3.8  $\mu$ mol) and Na/Hg (8  $\mu$ L of 0.5 M amalgam, 4  $\mu$ mol of Na) in a nitrogen glovebox. On a high-vacuum line, the tube was evacuated to remove all nitrogen. THF- $d_8$  was put through several freeze–pump–thaw cycles to remove all nitrogen. A small amount (0.5 mL) of THF- $d_8$  was then added by vacuum transfer to the NMR tube. The solution was allowed to react for approximately 1 h, with periodic shaking. A slightly cloudy yellow brown solution was formed. The  $^1H$  NMR spectrum of **7** matches that reported in the literature.

**Addition of Hydrogen to  $Cp^*_2TaCl(THF-d_8)$  (**7**).** Hydrogen (ca. 1 atm) was added to a frozen sample (77 K) of **7** in THF- $d_8$  (ca. 8 mM). Upon warming to room temperature, the reaction was monitored by  $^1H$  NMR spectroscopy. Within 1 h at room temperature, all starting material was consumed and a single product,  $Cp^*_2TaH_2Cl$  (**9**), was observed. Over time,  $Cp^*_2TaH_2Cl$  (**8**) was formed, as well as two other products,  $Cp^*_2Ta(=O)H$  (**10**) [ $\delta$  1.98 (s, 30H,  $C_5CH_3$ ), and 7.0 (s, 1H, Ta–H)] and  $Cp^*_2TaHCl_2$  (**11**) [ $\delta$  2.02 (s, 30H,  $C_5CH_3$ ), and 12.2 (s, 1H, Ta–H)]. Complexes **10** and **11** were assigned on the basis of comparison to benzene- $d_6$  spectra of these species and integration of the THF- $d_8$  spectra, and their formation is likely due to some water contamination, as discussed for the reactions of **6** in benzene- $d_6$  (Scheme 2). The four species **8**, **9**, **10**, and **11**, were present in nearly equivalent amounts after 12 h at room temperature.

**Addition of CO to  $(Cp^*_2TaCl)_2(\mu-N_2)$  (**6**).** A resealable NMR tube with a J. Young valve was charged with **6** (1 mg) and dry benzene- $d_6$  (ca. 0.5 mL) in a nitrogen-atmosphere glovebox. The tube was frozen in liquid nitrogen and evacuated on a high-vacuum line, then CO (ca. 1 atm) was added to the tube. Upon warming to room temperature, the reaction was monitored by  $^1H$  NMR spectroscopy. After 18 h at room temperature followed by 8 h at 45 °C, all of the starting material had been consumed and the  $^1H$  NMR spectrum showed a single resonance at  $\delta$  1.68, which corresponds to the known complex  $Cp^*_2Ta(CO)Cl$ .<sup>11</sup>

**Acknowledgment.** We thank the National Science Foundation (Grant CHE-0092446) for support of this work. We also want to thank Dr. James Houllis and Mr. David Filmore for preliminary work on this study.

**Supporting Information Available:** Full crystallographic data for **6** in CIF format. This material is available free of charge via the Internet at <http://pubs.acs.org>.

IC025578J

(17) The SADABS absorption correction program is based on the method of Blessing; see: Blessing, R. H. *Acta Crystallogr., Sect. A* **1995**, *51*, 33–38.

(18) *SHELXTL*: Structure Analysis Program, version 5.04; Siemens Industrial Automation Inc.: Madison, WI, 1995.